Journal of Magnetism and Magnetic Materials 478 (2019) 116–121

Contents lists available at ScienceDirect

Journal of Magnetism and Magnetic Materials

journal homepage: www.elsevier.com/locate/jmmm

Research articles

A novel $FeCoNiCr_{0.2}Si_{0.2}$ high entropy alloy with an excellent balance of mechanical and soft magnetic properties

Hang Zhang[a], Yaoxuan Yang[a], Lei Liu[a], Chen Chen[a], Tan Wang[a], Ran Wei[a], Tao Zhang[b], Yaqiang Dong[c], Fushan Li[a,*]

[a] School of Materials Science and Engineering, Zhengzhou University, Zhengzhou 450001, China
[b] Key Laboratory of Aerospace Materials and Performance (Ministry of Education), School of Materials Science and Engineering, Beihang University, Beijing 100191, China
[c] Zhejiang Province Key Laboratory of Magnetic Materials and Application Technology, CAS Key Laboratory of Magnetic Materials and Devices, Ningbo Institute of Materials Technology & Engineering, Chinese Academy of Sciences, Ningbo, Zhejiang 315201, China

ARTICLE INFO

Keywords:
High entropy alloy
Soft magnetic properties
Mechanical properties
Low coercivity
Rolling deformation

ABSTRACT

A novel $FeCoNiCr_{0.2}Si_{0.2}$ (at. %, thereafter, all mean atomic ratios) high-entropy alloy (HEA) was synthesized. The as-cast HEA exhibits a combination of excellent mechanical and magnetic properties with a large plastic deformation of about 60% and low coercivity (H_c) of about 187.9 A/m, which are prominent in the HEAs reported so far. Based on the large plasticity, rolling and annealing were adopted as a strategy for improving magnetic and mechanical properties of the HEA. The process of rolling followed by annealing leads to the significant enhancement of the yield strength (YS) and ultimate tensile strength (UTS) of alloy rolled at 773 K, increasing to 320 and 920 MPa respectively. Meanwhile the large plasticity and good soft magnetic properties remain. The enhancement mechanism of annealed after rolling was analyzed. Consequently, the optimal balance of magnetic and mechanical properties is achieved. The present work suggests a promising way to develop HEAs with a combination of excellent magnetic and mechanical properties.

1. Introduction

The emergence of high entropy alloys (HEAs) provided a new alloy design concept [1,2]. Generally, HEAs contain at least five principal elements with concentration between 5 and 35 at. %, which is different from traditional alloys containing one or two principal elements, and is beneficial for broadening the compositional range of alloys. Recent studies further extended the boundary of HEAs by categorizing quaternary and ternary alloy system with moderate component and solid solution structure into HEAs [3–5]. HEAs tend to form single-phase solid solutions rather than intermetallics, which is commonly regarded to be resulted from high entropy effect [6,7]. The properties of HEAs such as their high strength, excellent room-temperature ductility, good thermal stability and high electrical resistivity have been investigated extensively [4,8–14]. From the view of tuning coupled structural-magnetic transition, Huang et al. put forward a systematic study of the Curie temperature (T_c) for a number of equiatomic medium- and high-entropy alloys using first-principle theory, which are helpful to identify promising magnetic compositions [15].

As soft magnetic materials, a good balance of magnetic and mechanical properties is vitally important. Among current magnetic materials, silicon steel and Fe-based amorphous alloy have been treated as two kinds of desired core materials. However, owing to the intrinsically limited ductility and formability of 6.5 wt% Si electrical steel [16], it is extremely hard to be manufactured by conventional thick-slab casting and rolling process. And Fe-based amorphous alloy has not the ability of rolling deformation due to their lack of ductility. A series of FeCoNi-containing HEAs with excellent mechanical properties and promising ferromagnetic properties have been developed in recent years [17–20], among which FeCoNiSiB [18,21], $FeCoNi(AlSi)_{0.2}$ [22] and FeCoNiCrAl [23] HEAs show relatively high saturated magnetization (M_s) and malleability. Moreover, the FeCoNi-containing HEAs usually exhibit high thermal stability at elevated temperatures, which provides a great opportunity to be utilized as high-temperature magnetic material [26–28]. High ductility of HEAs can greatly overcome the formability limit of silicon steel. However, the H_c of FeCoNi-containing HEAs currently developed is obviously higher than those of Fe-based amorphous alloy and even silicon steel, which remains a challenge for future practical applications. Therefore, more investigations deserve to be conducted on developing new HEAs with both excellent

* Corresponding author.
E-mail address: fsli@zzu.edu.cn (F. Li).

https://doi.org/10.1016/j.jmmm.2019.01.096
Received 25 October 2018; Received in revised form 3 January 2019; Accepted 27 January 2019
Available online 28 January 2019
0304-8853/

malleability and low H_c.

In the present study, a novel $FeCoNiCr_{0.2}Si_{0.2}$ HEA is developed with the aim of obtaining a good balance of improved soft magnetic properties, excellent mechanical properties and high structural stability. Rolling and annealing, widely used as a formability route, were introduced as a strategy for improving magnetic and mechanical properties in the present work.

2. Experimental procedure

Alloy ingots with nominal composition of $FeCoNiCr_{0.2}Si_{0.2}$ (at. %) were prepared by arc melting the mixtures of Fe, Co, Ni, Cr and Si (purity above 99.9 wt%) in a water-cooled Cu crucible under Ti-gettered argon atmosphere. The ingots were re-melted 5 times to ensure chemical homogeneity. The plates with 75 mm × 30 mm × 6 mm were produced by the casted method of tilt-pour steel mold casting. The plates were deformed by multi-pass hot rolling at 773 K to thickness strain of 59%. Then the rolled samples were isothermally annealed at 1273 K for 1 h.

The structure was examined by X-ray diffractometer (XRD, Empyrean) with Cu-Kα radiation. Thermal stability was studied by differential scanning calorimetry (DSC, NETZSCH 404) at a heating rate of 20 K/min. The curie transition was determined by thermomagnetic measuring instrument (TGA5500) at a heating speed of 20 K/min. The room-temperature Vickers hardness (HV) was measured with a load of 3 N, and at least 8 points were tested on each sample. The magnetic properties including M_s and H_c were measured with vibrating sample magnetometer (VSM, Lake Shore 7410) and B-H loop tracer (EXPH-100), respectively. All the measurements were performed at room temperature. Samples for tensile tests with a cross-section of 2 mm × 1.5 mm and a gauge length of 10 mm were cut by electro-discharge machining. Fracture surfaces of tensile samples were examined by scanning electron microscopy (SEM, FEI QUANTA 200), and crystallographic textures were quantified by electron backscatter diffraction (EBSD, JEM 7500).

3. Results

Fig. 1 shows the XRD patterns of as-cast, as-rolled and annealed after rolling $FeCoNiCr_{0.2}Si_{0.2}$ HEA. Only FCC phase could be detected in the three statuses, indicating that no phase transformation occurred during hot rolling and annealing. Generally, the introduction of deformation and stress during repeatedly rolling can lead to broadening and shifting of diffraction peak. But it is interesting and abnormal that the present alloy does not exhibit this behavior, which is similar to that

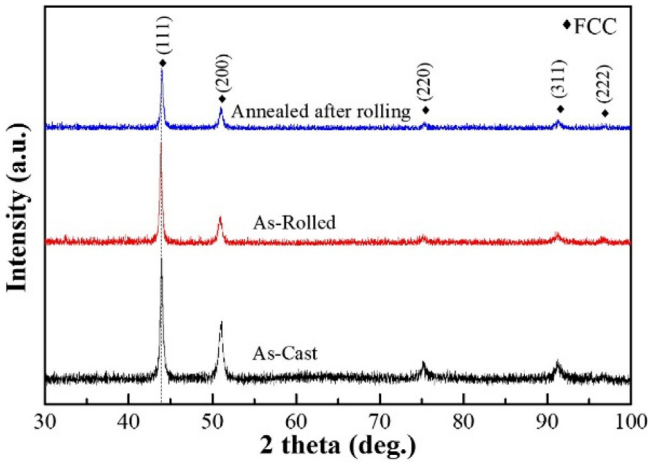

Fig. 1. XRD patterns of the as-cast, as-rolled and annealed after rolling $FeCoNiCr_{0.2}Si_{0.2}$ HEA.

Table 1
The crystal structure, lattice parameter, Curie temperature (T_c), Vickers hardness (HV), saturated magnetization (M_s), coercivity (H_c), yield strength (YS), ultimate tensile strength (UTS), elongation-to-fracture (EL) and UTS × EL for the as-cast, as-rolled and annealed after rolling $FeCoNiCr_{0.2}Si_{0.2}$ HEA.

Characteristics	As-Cast	As-Rolled	Annealed after rolling
Structure	FCC	FCC	FCC
Lattice parameter (Å)	3.5689	3.5742	3.5690
T_c (K)	702.57	711.72	704.42
HV	130.1	318.2	153.8
M_s (emu/g)	98.11	102.96	98.33
H_c (A/m)	187.9	298.2	186.3
YS (MPa)	225	705	320
UTS (MPa)	732	1070	920
EL (%)	61	10	60
UTS × EL (GPa %)	44.6	10.7	55.2

reported by Liu [24]. This feature is very different from the most of current HEAs and traditional alloys, such as $FeCoCr_{0.5}Ni$ [25] and AlCoCrFeNi [26]. The lattice parameters are calculated from the XRD results and summarized in Table 1. This phenomenon suggests that the lattice parameters of this alloy are very stable to variations of stress and temperature, though it needs to be further studied.

The thermal stability was investigated by DSC. The DSC curves of as-cast, as-rolled and annealed after rolling $FeCoNiCr_{0.2}Si_{0.2}$ HEA is shown in Fig. 2(a). The alloy in all the states exhibits a similar trend of slowly exothermic change in the temperature range of 473–1273 K [27]. There is no endothermic line occurring, indicating that there is no occurrence of phase transformation or collapse of crystalline structure even under the high temperature [27]. It is clear that all the alloy of as-cast, as-rolled and annealed after rolling are stable under the temperature below 1273 K. The as-rolled sample shows more prominent exothermic behavior than that of as-cast sample, due to the internal stress induced by rolling. Upon annealing, the exothermic behavior of the rolled alloy reduces, which is attributed to internal stress relief to a certain extent. Furthermore, Fig. 2(b) shows the thermomagnetic cures of the as-cast, as-rolled and annealed after rolling $FeCoNiCr_{0.2}Si_{0.2}$ alloy. The T_c is determined to be around 700 K. The T_c of as-cast and annealed samples has not changed obviously. Compared to the annealed after rolling and as-cast samples, as-rolled sample has a slightly higher T_c.

EBSD technique was taken to better understand texturing evolution during heat treatment processing. The as-cast sample of the HEA has equiaxed coarse grains with a grain size range from 10 to 217 μm, as shown in Fig. 3(a) and (b). It has a single solid solution phase with FCC structure, consistent with the XRD results shown in Fig. 1. The grains gradually become elongated in the rolling direction, as shown in Fig. 3(d) and (e), taking on a blurry structure, in which the boundaries are hard to distinguish. And the color orientation within the grains increases significantly, indicating more fragmented grains than that in the as-cast structure. Fig. 3(g) and (h) show inverse pole figure (IPF) of the HEA processed by hot-rolling followed by annealing at 1273 K for 1 h. As a result, the recrystallized and fine-grained structure forms and the grain size falls into the scale between 7 and 39 μm, and distribution of grain diameter is more uniform as shown in Fig. 3(c), (f) and (i). Both the as-rolled and annealed after rolling alloy show a single FCC phase structure and no occurrence of new phase formation, implying high structural stability.

Fig. 4(a) gives the tensile engineering stress-strain curves of the as-cast, as-rolled and annealed after rolling samples. The YS, UTS and elongation-to-fracture (EL) are listed in Table 1. The as-cast sample shows excellent ductility with plastic strain of 61%, but its YS is only 225 MPa. The rolled alloy has a remarkable increase in the yield and fracture strength but at the cost of ductility. A good balance among YS, UTS and EL was achieved in the annealed after rolling sample with 320 MPa, 920 MPa and 60%, respectively. It is of significance that,

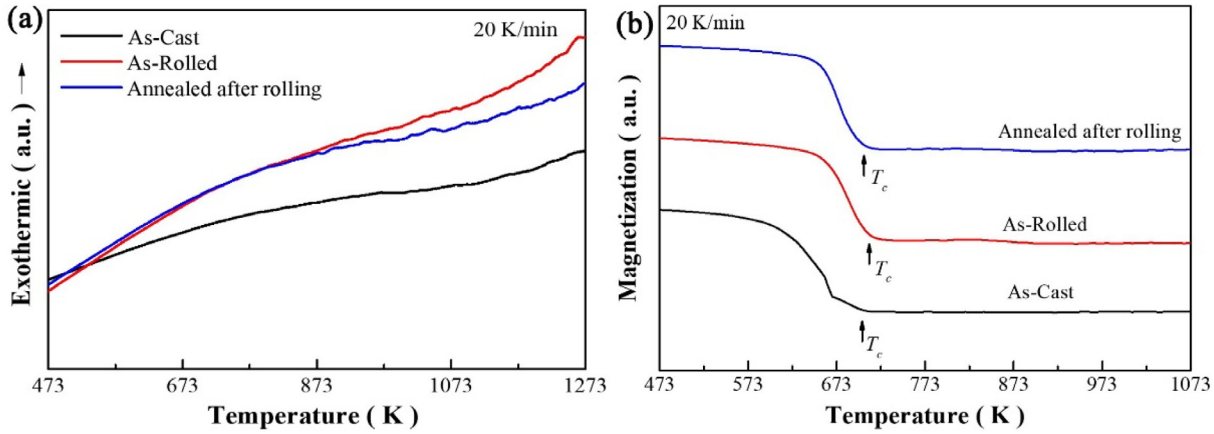

Fig. 2. DSC curves (a) and thermomagnetic curves (b) of the as-cast, as-rolled and annealed after rolling $FeCoNiCr_{0.2}Si_{0.2}$ HEA.

compared with casting, the annealed after rolling process greatly enhances the YS and EL. The fractured surfaces of the as-cast, rolled and annealed after rolling $FeCoNiCr_{0.2}Si_{0.2}$ HEA are shown in Fig. 4(b-g). Macroscopically, significant necking occurs in the as-cast and annealed after rolling samples with typical, while fracture morphology without obviously necking tendency was observed only in the rolled sample as shown in Fig. 4(b), (d) and (f). It is observed that the only rolled sample shows a brittle fracture morphology with river shape and smaller dimples than that of the as-cast alloy as shown in Fig. 4(c) and (e). After further annealed, a ductile fracture feature appears on the fracture surface of the rolled sample with dimples, which is similar to that of the as-cast one, seeing Fig. 4(g). The fractography of the annealed after rolling sample implies high working hardening ability and large plasticity, i.e. large the value of damage tolerance (UTS × EL), which is consistent with the results obtained by tensile test.

Fig. 5(a) gives Hysteresis loops of the as-cast, rolled and annealed after rolling $FeCoNiCr_{0.2}Si_{0.2}$ HEA. All the samples exhibit typical soft magnetic characteristics. The M_s of the present HEA remains unchanged basically after processes by rolling and annealing technique. However, the H_c of the alloy increases from 187.9 to 298.2 A/m after rolling. After further annealed, it reduces to 186.3 A/m, which is close to that of the as-cast state. Fig. 5 (b) shows the statistic results for the M_s and H_c of different soft magnets in HEAs [22,28–33], and it notes that $FeCoNiCr_{0.2}Si_{0.2}$ HEA exhibits excellent combination of high M_s and low H_c.

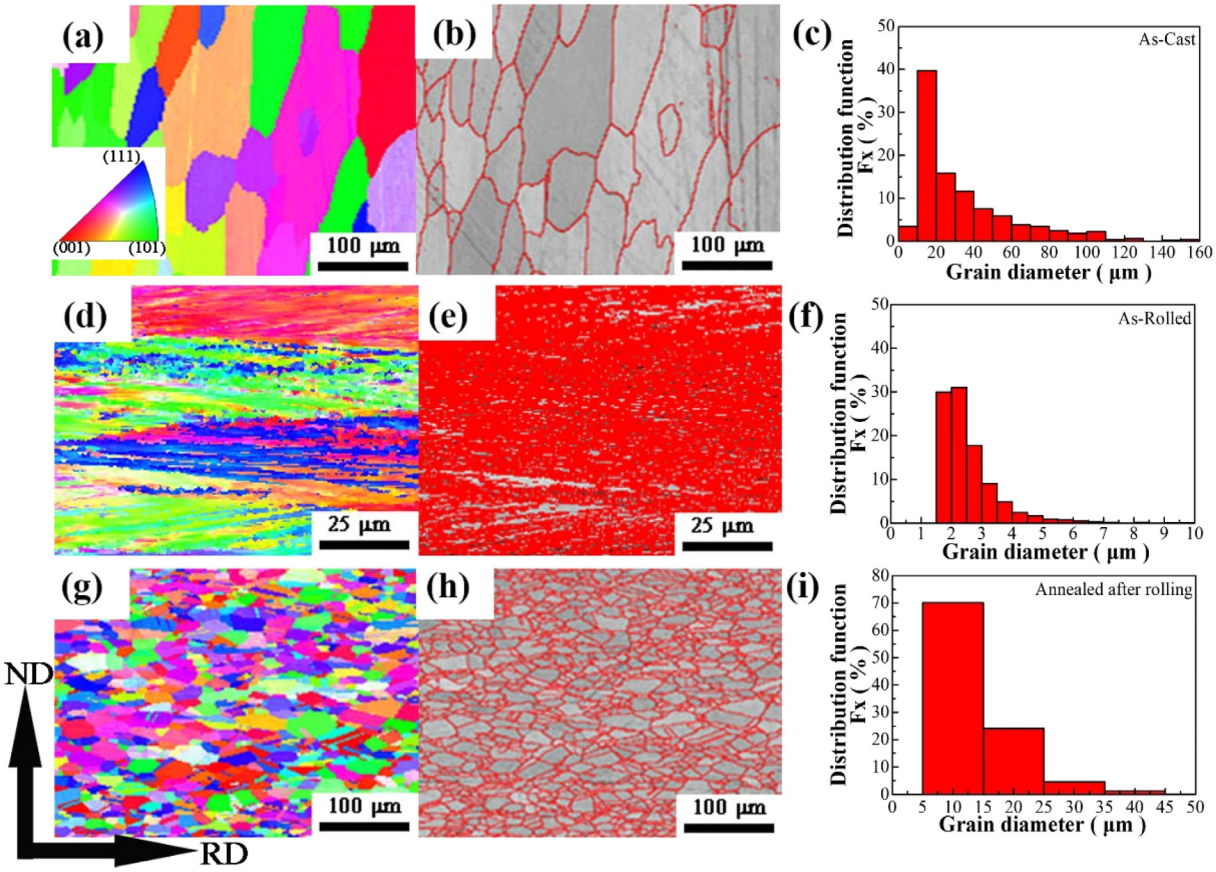

Fig. 3. Inverse pole figure (IPF) maps of $FeCoNiCr_{0.2}Si_{0.2}$ HEA with different statuses: (a) as-cast, (d) as-rolled and (g) annealed after rolling. Color-coding refers to the grain orientations. Grain boundary (GB) maps of $FeCoNiCr_{0.2}Si_{0.2}$ HEA with different statuses: (b) as-cast, (e) as-rolled and (h) annealed after rolling. And distribution maps of grain diameter of $FeCoNiCr_{0.2}Si_{0.2}$ HEA with different statuses: (c) as-cast, (f) as-rolled and (i) annealed after rolling.

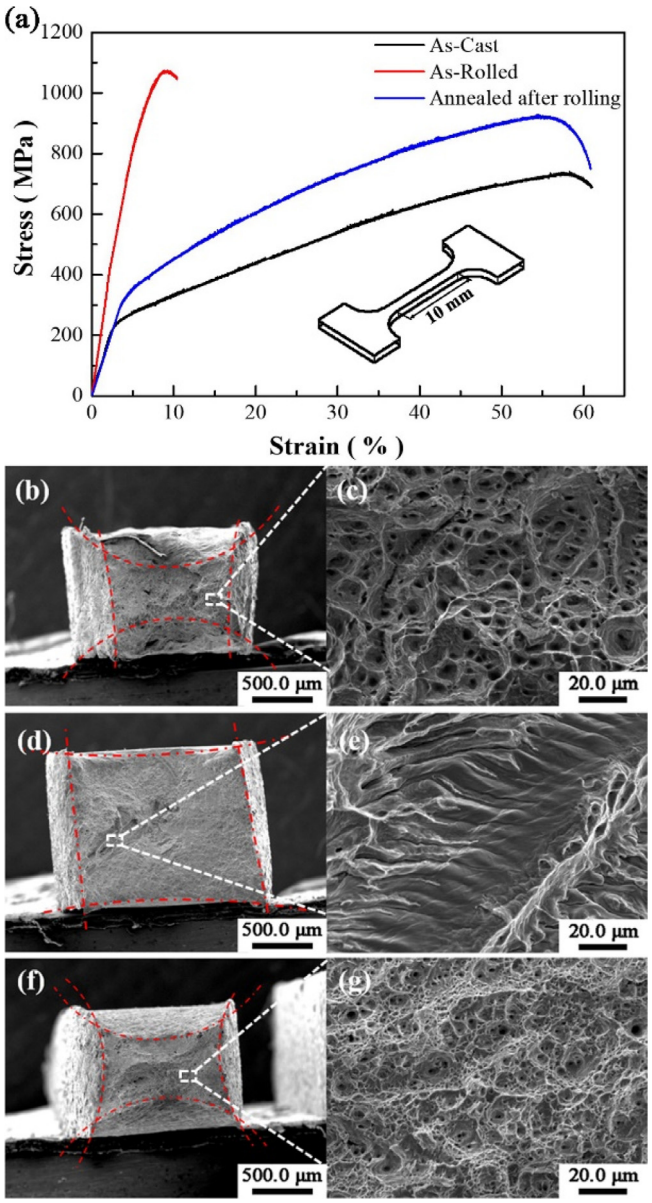

Fig. 4. Tensile engineering stress-strain curves (a) of the as-cast, as-rolled and annealed after rolling $FeCoNiCr_{0.2}Si_{0.2}$ HEA. Fracture surfaces of the as-cast (b) and (c), as-rolled (d) and (e), and annealed after rolling (f) and (g) $FeCoNiCr_{0.2}Si_{0.2}$ HEA at low and high magnification, respectively.

4. Discussion

Previous work indicates that the T_c of HEAs is sensitive to their base composition, additional alloying elements, and crystal structure [15,31,34]. For the present HEA, T_c becomes slightly higher after rolling, which is similar to the result achieved by Lucas et al. in FeCoCrNi HEA [25]. And the possible reason is that both the as-cast and annealed after rolling samples have some degree of short-range chemical ordering, but the rolled sample is chemically disordered during the mechanical processing. Chemical disordered structure tends to correspond to high T_c [25].

The good balance among YS, UTS and EL is achieved in the annealed after rolling sample of $FeCoNiCr_{0.2}Si_{0.2}$ HEA, which results from the formation of the recrystallized fine-grained and uniform structure with the average grain diameter of 12.8 μm. It is well known from Hall-Petch effect that the YS has inversely proportional correlation to the mean grain size. When the fine grain is forced to be deformed, the stress can be dispersed by multiple grain boundaries, leading to more uniform plastic deformation with less stress concentration, and the extension of cracks would be well hindered. Thus, the major contributor to strengthening in this work reasonably originates from the grain refinement. According to the Hall-Petch relationship, $\sigma = \sigma_0 + k_{HP} d^{-1/2}$, the lattice friction ($\sigma_0$) and strengthening coefficient (K_{HP}) for the $FeCoNiCr_{0.2}Si_{0.2}$ HEA have been estimated to be about 140 MPa and 643 MPa·μm$^{1/2}$, respectively. Most of the mechanical properties reported for HEAs are based on hardness measurements and uniaxial compression tests [2,35–41]. The parameter K_{HP} of tensile test from the current study and many other FCC alloys was just summarized in Table 2. Through the comparison and analysis of data, strengthening is not only determined by the number of constituent elements but also depends on the type of added elements. In the present family of alloys, Cr appears to be the most potent strengthener [42].

Because the properties of plasticity and strength are evidently mutually exclusive in almost all classes of materials, the fundamental difficulty in finding high UTS × EL materials is still to strike a desirable balance between the strength and plasticity of the material [47]. Nevertheless, for $FeCoNiCr_{0.2}Si_{0.2}$ HEA processed by rolling and annealing, the value of (UTS-YS)/EL is much higher than that of the as-cast one, indicating that the alloy has good uniform deformation and extremely high work-hardening properties. In addition, the UTS × EL of the annealed samples reached 55 GPa%, which is much higher than that of the as-cast sample. It is of great significance that the value of UTS × EL of this alloy treated like this is one of the highest among reported HEAs [9,48,49].

Researches have shown that the H_c is inversely proportional to the average grain size, and the H_c is proportional to internal stress [50]. After rolling, the grains become fine and the grain boundaries of the alloy become indistinct, and there are various defects and internal stress inside the rolled alloy, leading to pinning effects that impede the movement of domain walls, thus the resultant H_c becomes extremely large. After annealed, only compared to rolled sample, the grain shape significantly changes and the distribution of grain diameter is more uniform, while the internal stress decreases. As a result, the magnetic isotropy increases and the movement resistance of domain walls decreases making the displacement of magnetic domain reversible, which favors the decrease in H_c. These results are consistent with the aforementioned microstructure, as shown in Fig. 3. The M_s of the material depend on the number of the atomic magnetic moment in unit volume, which is mainly affected by the composition of the material. Once the required composition of the material is determined, the change of microstructure would influence the M_s. It could be found from the XRD results in Fig. 1 that the phase microstructure remains unchanged regardless of rolling or annealing and thus no obvious change in M_s for the samples is exhibited, as shown in Fig. 5(a).

Compared with the currently developed FeCoNi-containing HEAs, although the magnetic moment of Cr is anti-parallel with Fe/Co/Ni, the present $FeCoNiCr_{0.2}Si_{0.2}$ alloy exhibits only a little lower M_s than $FeCoNi(AlSi)_{0.2}$ and is very close to $FeCoNi(MnAl)_{0.25}$, but the H_c of $FeCoNiCr_{0.2}Si_{0.2}$ is the lowest. The H_c is sensitive to the lattice distortion and the various microstructures. Lattice distortion affects the magnetic domain-wall movement and H_c. The atomic radii of Al and Mn are larger than that of Fe, Co and Ni, while atomic radius of Cr is similar to Fe, Co and Ni. Compared to $FeCoNi(AlSi)_{0.2}$ and $FeCoNi(MnAl)_{0.25}$, the lattice distortion of $FeCoNiCr_{0.2}Si_{0.2}$ is probably the smallest. This reasonably explains the reason for the lowest H_c obtained in the present $FeCoNiCr_{0.2}Si_{0.2}$, as shown in Fig. 5(b). Nevertheless, our result suggests that $FeCoNiCr_{0.2}Si_{0.2}$ is a promising candidate for soft magnetic applications than $FeCoNi(AlSi)_{0.2}$ [22] and $FeCoNi(MnAl)_{0.25}$ [24].

5. Conclusion

In summary, $FeCoNiCr_{0.2}Si_{0.2}$ HEA developed in this work was prepared by casting and processed by rolling and recrystallization

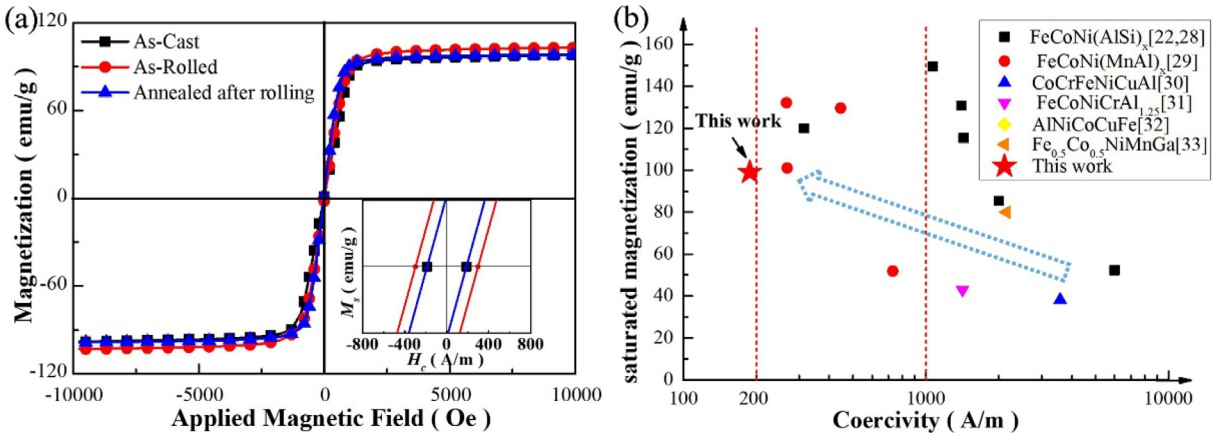

Fig. 5. Hysteresis loops of the as-cast, as-rolled and annealed after rolling $FeCoNiCr_{0.2}Si_{0.2}$ HEA (a) and the saturated magnetization and coercivity of the HEA (marked by pentagram) compared with other HEAs (b).

Table 2
The Hall-Petch coefficient (K_{HP}) of typical HEAs.

Alloy system	Structure	K_{HP} (MPa·μm$^{1/2}$)	Refs.
$CoCrFeNiAl_{0.1}$	FCC	371	[43]
$CoCrFeNiAl_{0.3}$	FCC	730	[44]
CoCrFeMnNi	FCC	494	[45]
FeNiCoCr	FCC	855	[42]
CoCrNi	FCC	568	[46]
$FeCoNiCr_{0.2}Si_{0.2}$	FCC	643	This work

annealing route. Structural, thermal, magnetic and mechanical properties of the alloys were investigated and compared. Major conclusions of this work are drawn as follows:

1. The good balance of improved soft magnetic properties and excellent mechanical properties is obtained in novel $FeCoNiCr_{0.2}Si_{0.2}$ HEA. The plastic deformation of the HEA is near to 60%. The H_c of the alloy is much lower than most of the previously reported HEAs, which is of great significance for practical application.
2. The excellent ductility and formability of the alloy HEA make rolling and annealing a strategy for improving magnetic and mechanical properties. After processed by rolling and recrystallization annealing, the strength and plasticity are greatly increased. Especially, the value of UTS × EL reaches 55 GPa%, which is the one of the highest values in HEAs.
3. The as-cast $FeCoNiCr_{0.2}Si_{0.2}$ HEA is comprised of a simple FCC solid solution structure, which is quite stable to deformation and high temperature. After rolling and annealing, no new phase was detected by XRD.

Acknowledgements

The work was supported by National Natural Science Foundation of China [grant numbers U1704159, 51701183]; China Postdoctoral Science Foundation funded project [grant numbers 2017M622368, 2018M630834]; and Henan Technical Innovation Guidance projects [grant number 182107000050].

Appendix A. Supplementary data

Supplementary data to this article can be found online at https://doi.org/10.1016/j.jmmm.2019.01.096.

References

[1] B. Cantor, I.T.H. Chang, P. Knight, A.J.B. Vincent, Mater. Sci. Eng. A 375–377 (2004) 213–218.
[2] J.W. Yeh, S.K. Chen, S.J. Lin, J.Y. Gan, T.S. Chin, T.T. Shun, C.H. Tsau, S.Y. Chang, Adv. Eng. Mater. 6 (2004) 299–303.
[3] M.S. Lucas, G.B. Wilks, L. Mauger, J.A. Munoz, O.N. Senkov, E. Michel, J. Horwath, S.L. Semiatin, M.B. Stone, D.L. Abernathy, E. Karapetrova, Appl. Phys. Lett. 100 (2012).
[4] T.T. Zuo, R.B. Li, X.J. Ren, Y. Zhang, J. Magn. Magn. Mater. 371 (2014) 60–68.
[5] W. Guo, W. Dmowski, J.Y. Noh, P. Rack, P.K. Liaw, T. Egami, Metall. Mater. Trans. A 44A (2013) 1994–1997.
[6] Y. Zhang, T.T. Zuo, Z. Tang, M.C. Gao, K.A. Dahmen, P.K. Liaw, Z.P. Lu, Prog. Mater. Sci. 61 (2014) 1–93.
[7] C.J. Tong, Y.L. Chen, S.K. Chen, J.W. Yeh, T.T. Shun, C.H. Tsau, S.J. Lin, S.Y. Chang, Metall. Mater. Trans. A 36A (2005) 881–893.
[8] Z.H. Han, S. Liang, J. Yang, R. Wei, C.J. Zhang, Mater. Charact. 145 (2018) 619–626.
[9] R. Wei, H. Sun, Z.H. Han, C. Chen, T. Wang, S.K. Guan, F.S. Li, Mater. Lett. 219 (2018) 85–88.
[10] L.B. Chen, R. Wei, K. Tang, J. Zhang, F. Jiang, L. He, J. Sun, Mater. Sci. Eng. A 716 (2018) 150–156.
[11] Y.X. Ye, C.Z. Liu, H. Wang, T.G. Nieh, Acta Mater. 147 (2018) 78–89.
[12] O.N. Senkov, S.V. Senkova, C. Woodward, Acta Mater. 68 (2014) 214–228.
[13] J.E. Saal, I.S. Berglund, J.T. Sebastian, P.K. Liaw, G.B. Olson, Scripta Mater. 146 (2018) 5–8.
[14] B. Gludovatz, A. Hohenwarter, D. Catoor, E.H. Chang, E.P. George, R.O. Ritchie, Science 345 (2014) 1153–1158.
[15] S. Huang, E. Holmström, O. Eriksson, L. Vitos, Intermetallics 95 (2018) 80–84.
[16] H.Z. Li, H.T. Liu, Y. Liu, Z.Y. Liu, G.M. Cao, Z.H. Luo, F.Q. Zhang, S.L. Chen, L. Lyu, G.D. Wang, J. Magn. Magn. Mater. 370 (2014) 6–12.
[17] R. Wei, H. Sun, C. Chen, Z. Han, F. Li, J. Magn. Magn. Mater. 435 (2017) 184–186.
[18] R. Wei, H. Sun, C. Chen, J. Tao, F. Li, J. Magn. Magn. Mater. 449 (2018) 63–67.
[19] T. Zuo, M.C. Gao, L. Ouyang, X. Yang, Y. Cheng, R. Feng, S. Chen, P.K. Liaw, J.A. Hawk, Y. Zhang, Acta Mater. 130 (2017) 10–18.
[20] M.C. Gao, D.B. Miracle, D. Maurice, X. Yan, Y. Zhang, J.A. Hawk, J. Mater. Res. (2018) 1–18.
[21] R. Wei, J. Tao, H. Sun, C. Chen, G.W. Sun, F.S. Li, Mater. Lett. 197 (2017) 87–89.
[22] Y. Zhang, T.T. Zuo, Y.Q. Cheng, P.K. Liaw, Sci. Rep. 3 (2013).
[23] S.G. Ma, Y. Zhang, Mater. Sci. Eng. A-Struct. 532 (2012) 480–486.
[24] P. Li, A. Wang, C.T. Liu, J. Alloy. Compd. 694 (2017) 55–60.
[25] M.S. Lucas, D. Belyea, C. Bauer, N. Bryant, E. Michel, Z. Turgut, S.O. Leontsev, J. Horwath, S.L. Semiatin, M.E. McHenry, C.W. Miller, J. Appl. Phys. 113 (2013).
[26] J.X. Hou, M. Zhang, S.G. Ma, P.K. Liaw, Y. Zhang, J.W. Qiao, Mater. Sci. Eng. A-Struct. 707 (2017) 593–601.
[27] N.H. Tariq, M. Naeem, B.A. Hasan, J.I. Akhter, M. Siddique, J. Alloy. Compd. 556 (2013) 79–85.
[28] T.T. Zuo, S.B. Ren, P.K. Liaw, Y. Zhang, Int. J. Miner. Metall. Mater. 20 (2013) 549–555.
[29] P.P. Li, A.D. Wang, C.T. Liu, Intermetallics 87 (2017) 21–26.
[30] K.B. Zhang, Z.Y. Fu, J.Y. Zhang, J. Shi, W.M. Wang, H. Wang, Y.C. Wang, Q.J. Zhang, J. Alloy. Compd. 502 (2010) 295–299.
[31] Y.F. Kao, S.K. Chen, T.J. Chen, P.C. Chu, J.W. Yeh, S.J. Lin, J. Alloy. Compd. 509 (2011) 1607–1614.
[32] R. Kulkarni, B.S. Murty, V. Srinivas, J. Alloy. Compd. 746 (2018) 194–199.
[33] T. Zuo, M. Zhang, P.K. Liaw, Y. Zhang, Intermetallics 100 (2018) 1–8.
[34] S. Huang, W. Li, X.Q. Li, S. Schonecker, L. Bergqvist, E. Holmstrom, L.K. Varga, L. Vitos, Mater. Des. 103 (2016) 71–74.
[35] W.H. Liu, Y. Wu, J.Y. He, T.G. Nieh, Z.P. Lu, Scripta Mater. 68 (2013) 526–529.
[36] B. Kang, J. Lee, H.J. Ryu, S.H. Hong, J. Alloy. Compd. 767 (2018) 1012–1021.
[37] R. Sriharitha, B.S. Murty, R.S. Kottada, J. Alloy. Compd. 583 (2014) 419–426.
[38] D. Wu, J.Y. Zhang, J.C. Huang, H. Bei, T.G. Nieh, Scripta Mater. 68 (2013) 118–121.
[39] Z. Wu, H. Bei, F. Otto, G.M. Pharr, E.P. George, Intermetallics 46 (2014) 131–140.
[40] R.S. Ganji, P.S. Karthik, K.B.S. Rao, K.V. Rajulapati, Acta Mater. 125 (2017) 58–68.

[41] B. Kang, J. Lee, H.J. Ryu, S.H. Hong, Mater. Sci. Eng. A-Struct. 712 (2018) 616–624.
[42] Z. Wu, H. Bei, G.M. Pharr, E.P. George, Acta Mater. 81 (2014) 428–441.
[43] N. Kumar, M. Komarasamy, P. Nelaturu, Z. Tang, P.K. Liaw, R.S. Mishra, Jom 67 (2015) 1007–1013.
[44] S.G. Ma, S.F. Zhang, J.W. Qiao, Z.H. Wang, M.C. Gao, Z.M. Jiao, H.J. Yang, Y. Zhang, Intermetallics 54 (2014) 104–109.
[45] F. Otto, A. Dlouhy, C. Somsen, H. Bei, G. Eggeler, E.P. George, Acta Mater. 61 (2013) 5743–5755.
[46] Y.L. Zhao, T. Yang, Y. Tong, J. Wang, J.H. Luan, Z.B. Jiao, D. Chen, Y. Yang, A. Hu, C.T. Liu, J.J. Kai, Acta Mater. 138 (2017) 72–82.
[47] M.D. Demetriou, M.E. Launey, G. Garrett, J.P. Schramm, D.C. Hofmann, W.L. Johnson, R.O. Ritchie, Nat. Mater. 10 (2011) 123–128.
[48] Z. Wang, I. Baker, Z. Cai, S. Chen, J.D. Poplawsky, W. Guo, Acta Mater. 120 (2016) 228–239.
[49] J.Y. He, H. Wang, H.L. Huang, X.D. Xu, M.W. Chen, Y. Wu, X.J. Liu, T.G. Nieh, K. An, Z.P. Lu, Acta Mater. 102 (2016) 187–196.
[50] C. Li, H. Ruan, D. Chen, K. Li, D. Guo, B. Shao, Microsc. Res. Tech. 81 (2018) 796–802.